

Phase-Controlled Phonon Laser

Yan-Lei Zhang,^{1,2} Chang-Ling Zou,^{1,2,3} Chuan-Sheng Yang,^{1,2} Hui Jing,^{4,*} Chun-Hua Dong,^{1,2} Guang-Can Guo,^{1,2} and Xu-Bo Zou,^{1,2†}

¹ Key Laboratory of Quantum Information, University of Science and Technology of China, Hefei 230026, People's Republic of China

² Synergetic Innovation Center of Quantum Information and Quantum Physics, University of Science and Technology of China, Hefei, Anhui 230026, China

³ Department of Applied Physics, Yale University, New Haven, Connecticut 06511, USA and

⁴ Key Laboratory of Low-Dimensional Quantum Structures and Quantum Control of Ministry of Education, Department of Physics and Synergetic Innovation Center for Quantum Effects and Applications, Hunan Normal University, Changsha 410081, China

(Dated: March 5, 2022)

A phase-controlled ultralow-threshold phonon laser is proposed by using tunable optical amplifiers in coupled-cavity-optomechanical system. Giant enhancement of coherent photon-phonon interactions is achieved by engineering the strengths and phases of external parametric driving. This in turn enables single-photon optomechanics and low-power phonon lasing, opening up novel prospects for applications, e.g. quantum phononics and ultrasensitive motion detection.

PACS numbers: 42.50.-p, 07.10.Cm, 42.65.-k

Introduction.- As a promising platform to study fascinating macroscopic quantum phenomena [1], cavity optomechanics [2, 3] has received tremendous attentions in recent years. All kinds of optomechanical couplings and applications [4] have been opened up due to remarkable experimental advances in e.g., mechanical ground-state cooling [5, 6], optomechanical non-reciprocity [7–9], optomechanically induced transparency [10, 11], nonclassical state preparation [12, 13], coherent state transfer between light and sound [14, 15], and various phonon-mediated hybrid devices [16]. To extend more applications, on the one hand, the unique regime of single-photon quantum optomechanics [18, 19], however, is still pursued in current experimental efforts; on the other hand, we need to realize convenient tuning, especially the switching between different optomechanical couplings.

To realize single-photon coupling, many theoretical schemes have been proposed based on, for examples, undriven two-cavity set-ups [20], optomechanical arrays [21], Josephson effect [22], and the transient scheme [23]. Very recently, the parametric drive has been used to enhance the nonlinear coupling [1, 2, 25] in optomechanical systems. By exploiting coupled cavities, many applications have been studied, such as single-photon generation [27], steady-state entanglement [28], thermal phonon squeezing [29], and phonon laser [30]. In the study of phononic devices [31–33], the phonon laser [34, 35] plays a key role in integrating coherent phonon sources, detectors, and waveguides [36]. Phonon lasing have been demonstrated in the electromechanical resonator [37], the nanomechanical resonator [38], the vertical cavity structure [39], and the compound microcavity system [40], and some schemes are also proposed to realize phonon laser in the quantum-dot system [41, 42]. In particular, the ultralow-threshold phonon laser [43, 44] still gives rise to the broad interest and remains largely unexplored.

In this paper, we present a scheme for both enhancing optomechanical couplings into the single-photon strong-coupling regime and realizing the switching between different optomechanical interactions using optical parametric amplifiers (OPAs). The key idea is to put two OPAs into both the auxiliary cavity and the optomechanical system, which leads to the squeezing of transformational optical modes. Due to the squeezing, we can obtain exponentially enhanced radiation-pressure, parametric amplification, and three-mode optomechanical couplings, which are controlled by the phase difference from the two OPAs. As one of applications, we study a phase-controlled ultralow-threshold phonon laser in detail. In addition, we consider the noise of the squeezed modes, which can be suppressed greatly via dissipative squeezing or an additional optical mode. With current experimentally accessible parameters, our scheme should be feasible to study quantum optomechanics.

Model.- We consider an optomechanical system with two coupled cavities, and each cavity contains a driven nonlinear optical medium for OPA, as shown in Fig. 1(a), which can be described by the Hamiltonian ($\hbar = 1$)

$$H = H_c + H_m + J \left(a_1 a_2^\dagger + a_1^\dagger a_2 \right), \quad (1)$$

$$H_c = \sum_j \omega_j a_j^\dagger a_j + \Lambda_j \left(a_j^{\dagger 2} e^{-i\Phi_{dj}} - i\omega_{dj} t + \text{H.c.} \right), \quad (2)$$

$$H_m = \omega_m b^\dagger b - g_0 a_2^\dagger a_2 (b^\dagger + b), \quad (3)$$

where a_j and b are the annihilation operators for the j th ($j = 1, 2$) cavity mode with frequency ω_j and the mechanical mode with frequency ω_m , respectively, and J is the photon-hopping interaction strength between two cavities. H_c describes the optical modes containing two different OPAs. H_m describes the optomechanical sys-

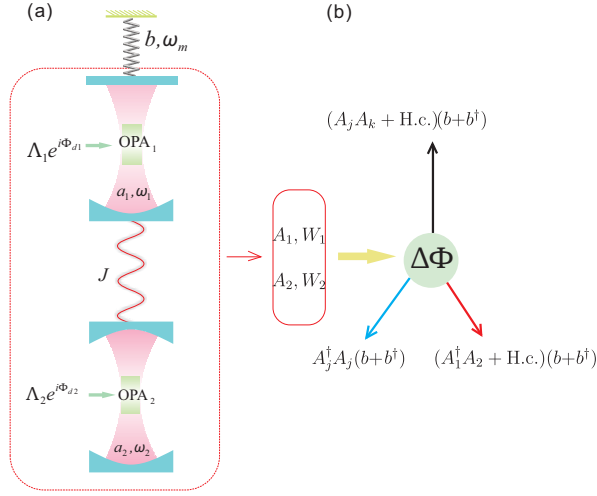


FIG. 1: (Color online) (a) Schematic diagram of the optomechanical system with coupled cavities. Each cavity contains an OPA with driving amplitude Λ_j , frequency ω_{dj} , and phase Φ_{dj} , respectively. The photon-hopping interaction J leads to the supermodes A_j with the frequency W_j . (b) The phase difference $\Delta\Phi = \Phi_{d1} - \Phi_{d2}$ controls the radiation-pressure $A_1^\dagger A_2 (b^\dagger + b)$, parametric amplification $(A_j A_k + \text{H.c.})(b^\dagger + b)$, and three-mode $(A_1^\dagger A_2 + \text{H.c.})(b^\dagger + b)$ optomechanical couplings.

tem associated with the 2nd cavity, in which g_0 is the radiation-pressure optomechanical coupling strength.

Phase-controlled optomechanical systems.- For simplicity, we take the two parametric driving frequencies satisfying $\omega_{d1} = \omega_{d2} = \omega_d$; then to diagonalize H_c , we define the squeezing operator a_{sj} via the transformation [1]:

$$a_j = \cosh(r_{dj}) a_{sj} - e^{-i\Phi_{dj}} \sinh(r_{dj}) a_{sj}^\dagger, \quad (4)$$

where $r_{dj} = (1/4) \ln [(\Delta_j + 2\Lambda_j) / (\Delta_j - 2\Lambda_j)]$ and $\Delta_j = \omega_j - \omega_d/2$, which requires $|\Delta_j| > 2\Lambda_j$ to avoid the system instability. Due to the photon-hopping, the transformational optical modes are coupled through the coherent term $\lambda_1 a_{s1} a_{s2}^\dagger + \text{H.c.}$ and squeezing term $\lambda_2 a_{s1} a_{s2} + \text{H.c.}$, in which $\lambda_{1,2}$ is the effective photon-hopping.

For convenient discussion, we define the effective coupling ratio between the squeezing and coherent terms $f_1 \equiv \left| \frac{\lambda_2(\omega_{s1} - \omega_{s2})}{\lambda_1(\omega_{s1} + \omega_{s2})} \right|$, where $\omega_{s1,2}$ is the frequency of the transformational optical mode $a_{s1,2}$. With the rotating wave approximation, it is obvious that we can reserve the squeezing (coherent) term for $f_1 \gg 1$ ($f_1 \ll 1$), which can be used to realize different optomechanical interactions.

When we have $f_1 \gg 1$, the squeezing term can be used to enhance optomechanical coupling strength [2], and we can further diagonalize the two-mode squeezing terms via the squeezing transformation ($j \neq k$)

$$a_{sj} = \cosh(r) A_j - e^{-i\Phi} \sinh(r) A_k^\dagger, \quad (5)$$

with A_j is the annihilation operator for the supermode j

with frequency $W_{j(k \neq j)} = \omega_{sj} \cosh^2(r) + \omega_{sk} \sinh^2(r) - \frac{|J'| \sinh(2r)}{2}$. The effective interaction Hamiltonian can be rewritten as

$$H_{int} = - \sum_{j=1}^2 G_j A_j^\dagger A_j (b^\dagger + b) + \sum_{j \leq k=1}^2 (G_{jk} A_j A_k + \text{H.c.})(b^\dagger + b) - (G_{p12} A_1^\dagger A_2 + \text{H.c.})(b^\dagger + b), \quad (6)$$

which describes the typical optomechanical forms including the radiation-pressure, parametric amplification, and three-mode optomechanical couplings. Here G_j is the effective coupling of optomechanical systems, where

$$G_1 = g_0 \cosh(2r_{d2}) \sinh^2(r), \quad (7)$$

$$G_2 = g_0 \cosh(2r_{d2}) \cosh^2(r), \quad (8)$$

with

$$r = \frac{1}{4} \ln \frac{\omega_{s1} + \omega_{s2} + |J'|}{\omega_{s1} + \omega_{s2} - |J'|}, \quad (9)$$

$$\frac{J'}{2J} = e^{i\Phi_{d2}} [\cosh(r_{d1}) \sinh(r_{d2}) + \cosh(r_{d2}) \sinh(r_{d1}) e^{i\Delta\Phi}], \quad (10)$$

depending on the phase difference $\Delta\Phi = \Phi_{d1} - \Phi_{d2}$. As illustrated in Fig. 1(b), the phase difference $\Delta\Phi$ determines the effective optomechanical couplings. As a comparison with the previous proposals [1, 2], the coupling G_j is greatly enhanced as the product of enhancement from the single-mode [1] and two-mode [2] squeezing. Here $\Phi = \arg(J')$ and the explicit expressions for the parameters $\lambda_{1,2}$, ω_{sj} , G_{jk} , and G_{p12} can be found in the Supplemental Material [45].

In Fig. 2(a), the optomechanical coupling strengths $G_{1,2}$ are plotted with reasonable parameters, which demonstrate the significant enhancement by controlling the phase $\Delta\Phi$ and show the strong-coupling regime is achievable (i.e. $G_1, G_2 \sim \omega_m > \kappa$) for $\Delta\Phi$ around the optimal $\Delta\Phi = \pi$. Because we choose the parametric pump detuning $\Delta_1 < 0$ and $\Delta_2 > 0$, which lead to $r_{d1} < 0$ and $r_{d2} > 0$, the effective $|J'|$ reaches its maximum when $\Delta\Phi = \pi$ and the minimum when $\Delta\Phi = 0$. In the Fig. 2(b), we plot the dependence of supermode frequencies $|W_1|/\omega_m, W_2/\omega_m$ on $\Delta\Phi$. When $\Delta\Phi$ tends to 0 or 2π , we have the coupling strength $G_2 \gg G_1$, while the other couplings G_{jk} and G_{p12} can be ignored for $|W_j + W_k \pm \omega_m| \gg G_{jk}$ and $|W_1 - W_2 \pm \omega_m| \gg G_{p12}$. To show the enhanced coupling strengths for different driving amplitude Λ_1 and phase $\Delta\Phi$, we plot the equipotential lines of $f_1, G_1/\omega_m, G_2/\omega_m$, and $\eta = G_1/G_2$ in the Fig. 2(c). The inner region surrounded by the blue line $f_1 = 10 \gg 1$ means that only the squeezing term

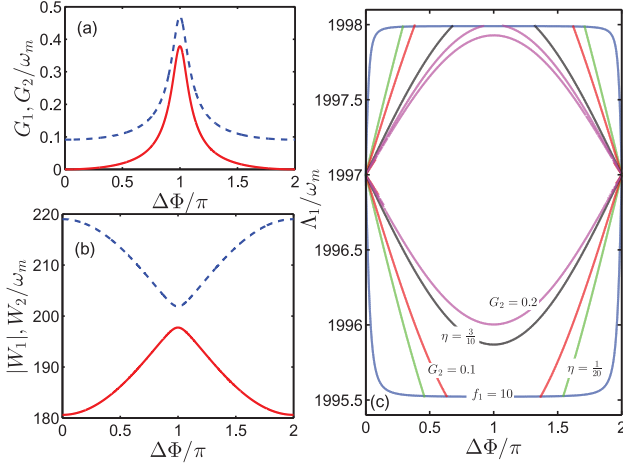


FIG. 2: (Color online) (a) The coupling G_1/ω_m (red-solid line) and G_2/ω_m (blue-dashed line) versus phase difference $\Delta\Phi$. (b) The supermodes $|W_1|/\omega_m$ (red-solid line) and $|W_2|/\omega_m$ (blue-dashed line) versus phase difference $\Delta\Phi$. The driving amplitude is $A_1 = 1997.96\omega_m$. (c) Equipotential lines versus A_1 and $\Delta\Phi$. The other parameters are $\Delta_1 = -4000\omega_m$, $\Delta_2 = 4000\omega_m$, $A_2 = 1997\omega_m$, $g_0 = 0.005\omega_m$, $J = 0.95\omega_m$, and $\kappa = 0.05\omega_m$.

dominates and the rotating wave approximation is appropriate. The red line $G_2 = 0.1\omega_m > \kappa$ and green line $\eta = \frac{1}{20}$ show that only the second optomechanical coupling reaches the strong-coupling regime. When the parameters A_1 and $\Delta\Phi$ tend to the central area, as shown by both the pink and black lines, both G_1 and G_2 can reach strong-coupling regime.

With appropriate parameters, the parametric amplification coupling forms in Eq. 6 can also be obtained when $\omega_m \gg G_j$ and $|W_1 - W_2 \pm \omega_m| \gg G_{p12}$, and meanwhile the frequency matching $|W_j + W_k \pm \omega_m| \approx 0$ is satisfied. The detailed discussion for the parametric amplification can be found in the Supplemental Material [45]. Compared to previous schemes that also employ the parametric interaction [46–48], the coefficient of parametric amplification is further improved by our coupled-cavity configuration, which can be used to generate photon-phonon pairs. Even when only one parametric driving field exists in the cavity, the optomechanical coupling can still be enhanced than no parametric driving [45].

Phase-controlled phonon laser.— The laser term in Eq. 6 could be utilized for realizing the phonon laser if G_{p12} is dominated over other coupling strengths. This interaction is a triply-resonant interaction, with the advantage that the pump and idle optical field are resonantly enhanced. When the triply-resonant frequency $W_1 - W_2 \approx \omega_m$ is matched, we have the parameter $f_1 \ll 1$. By a similar transformation [45] with the Eq. 5, we obtain

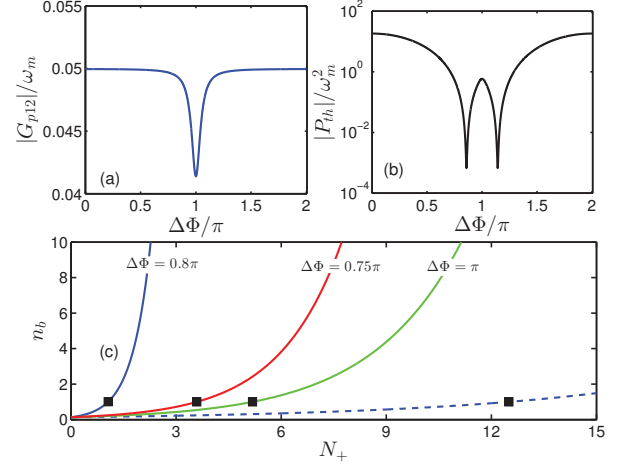


FIG. 3: (Color online) (a) The coupling $|G_{p12}|/\omega_m$ versus phase difference $\Delta\Phi$. (b) The threshold pump power P_{th}/ω_m^2 versus phase difference $\Delta\Phi$. (c) Plot of the stimulated emitted phonon number n_b as a function of the density of the supermode A_1 . The threshold density N_+ denoted by the black square points is obtained for $\mathcal{G} = \gamma_m$. The parameters are $\Delta_1 = 20\omega_m$, $\Delta_2 = 100\omega_m$, $A_1 = 9.94\omega_m$, $A_2 = 49.99\omega_m$, $J = 0.1\omega_m$, $g_0 = 0.002\omega_m$, $\kappa = 0.05\omega_m$, and $\gamma_m = 0.001\omega_m$.

$$G_{p12} = -\frac{g_0}{2} e^{-i\Phi} \cosh(2r_{d2}) \sin(\theta), \quad (11)$$

with $\Phi = \arg(J')$ and $\theta = \arctan[|J'|/(\omega_{s2} - \omega_{s1})]$, in which $J' = 2J[\cosh(r_{d1}) \cosh(r_{d2}) + \sinh(r_{d1}) \sinh(r_{d2}) e^{i\Delta\Phi}]$.

In Fig. 3(a), we plot the triply-resonant phonon lasing coupling strength $|G_{p12}|$ versus the phase difference $\Delta\Phi$, which can reach the strong-coupling regime $|G_{p12}| \simeq \kappa$, and there is no obvious change with the increasing of the phase difference. When the frequency matches $W_1 - W_2 \approx \omega_m$, we have $|G_j|/\omega_m$, $|G_{jk}|/(W_j + W_k \pm \omega_m) \ll 1$, therefore, the other coupling strengths can be neglected.

If the effective optical cavity decay rate exceeds the mechanical dissipation rate ($\kappa \gg \gamma_m$), we find the mechanical gain [40]

$$\mathcal{G} = \frac{|G_{p12}|^2 \Delta N \kappa}{(W_1 - W_2 - \omega_m)^2 + (\kappa/2)^2}, \quad (12)$$

where $\Delta N = N_+ - N_- \approx N_+$ with $N_+ = A_1^\dagger A_1$ and $N_- = A_2^\dagger A_2$. The gain has a spectral bandwidth κ and $W_1 - W_2 = \omega_m$ is corresponding to the maximum gain.

The threshold condition $\mathcal{G} = \gamma_m$ determines the emitted phonon number, which is shown in Fig. 3(c). The solid lines are stimulated emitted phonon number $n_b[\gamma_m] = \exp[2(\mathcal{G} - \gamma_m)/\gamma_m]$ as a function of the density N_+ for different $\Delta\Phi$. If there is no any OPA in the cavity, the emitted phonon number n_b with the resonance

$W_1 - W_2 = \omega_m$ is shown by the dashed line in Fig. 3(c). Clearly, it indicates an ultralow-threshold phonon laser by tuning the phase difference $\Delta\Phi$.

The black square points denote the threshold density N_+ for $\mathcal{G} = \gamma_m$ in Fig. 3(c). We know the threshold pump power as $P_{th} = N_+\kappa W_1$, and we obtain

$$P_{th} \approx \frac{\gamma_m W_1 \left[(W_1 - W_2 - \omega_m)^2 + (\kappa/2)^2 \right]}{|G_{p12}|^2}, \quad (13)$$

which is plotted as the function of phase difference $\Delta\Phi$ in Fig. 3(b). There are two dips, which mean an ultralow-threshold power with the near resonance $W_1 - W_2 \approx \omega_m$. The ultralow-threshold power P_{th} is related to the frequency difference $W_1 - W_2$ controlled by the strengths and phases of parametric driving terms. From the Fig. 3, it is noted that the threshold density $N_+ \leq 1$ can be obtained by changing the phase difference $\Delta\Phi$. In other words, the phonon lasing is possible with an ultralow-threshold power, as low as single photon.

Discussion.- In the presence of a parametric drive, the noise from the optical cavity decay might also be amplified. To circumvent the amplified noise, a possible strategy is to introduce a broadband single-mode or two-mode squeezed vacuum via dissipative squeezing [1, 2, 25]. This steady-state technique has recently been implemented experimentally [49–51], and recently it has been experimentally demonstrated that squeezed light can be used to cool the motion of a macroscopic mechanical object without resolved-sideband condition [52]. One can also take advantage of the tunability of the parametric drive to avoid significant perturbation of the initial photon state [25]. It is feasible to suppress the cavity noise in the experiment for realizing the optomechanical strong-coupling regime.

Conclusion.- we present a scheme for enhancing phase-controlled optomechanical couplings into the single-photon strong-coupling regime by optical squeezing. With two OPAs in two coupled optical cavities, we obtain the squeezing of transformational optical modes, which leads to exponentially enhanced optomechanical systems. The phase difference between the two driving fields on OPAs can control the enhanced radiation-pressure, parametric amplification, and three-mode optomechanical couplings. In particular, the three-mode optomechanical coupling can be used to realize a low-threshold phonon laser, and the threshold pump power is decreased greatly with the giant enhancement of mechanical gain. With current experimentally accessible parameters, our scheme should be feasible to study quantum optomechanics. This allows us to explore a number of interesting quantum optomechanics applications ranging from single-photon sources to nonclassical quantum states.

Acknowledgments. We thank Yue-Man Kuang, Xin-You Lü, Ya-Feng Jiao, and Jie-Qiao Liao for useful sug-

gestions. This work was funded by the National Key R & D Program (Grants No. 2016YFA0301300 and No. 2016YFA0301700), the National Natural Science Foundation of China (Grants No. 11474271, No. 11674305, and No. 61505195), and the China Postdoctoral Science Foundation (No. 2016M602013). H. J. is supported by the National Natural Science Foundation of China (Grants No. 11474087 and No. 11422437).

* Electronic address: jinghui73@gmail.com

† Electronic address: xbz@ustc.edu.cn

- [1] Yanbei Chen, J. Phys. B: At. Mol. Opt. Phys. **46**, 104001 (2013).
- [2] M. Aspelmeyer, P. Meystre, and K. Schwab, Phys. Today **65**, 29 (2012).
- [3] T. J. Kippenberg and K. J. Vahala, Science **321**, 1172 (2008).
- [4] M. Aspelmeyer, T. J. Kippenberg, and F. Marquardt, Rev. Mod. Phys. **86**, 1391 (2014).
- [5] J. D. Teufel et al., Nature **475**, 359 (2011).
- [6] Y.-S. Park, and H. Wang, Nature **5**, 489 (2009).
- [7] C.-H. Dong, Z. Shen, C.-L. Zou, Y.-L. Zhang, W. Fu, and G.-C. Guo, Nat. Commun. **6**, 6193 (2015).
- [8] Z. Shen, Y.-L. Zhang, Y. Chen, C.-L. Zou, X.-F. Xiao, X.-B. Zou, F.-W. Sun, G.-C. Guo, and C.-H. Dong, Nat. Photonics. **10**, 657 (2016).
- [9] J. Kim, M. C. Kuzyk, K. Han, H. Wang, and G. Bahl, Nat. Phys. **11**, 275 (2015).
- [10] S. Weis, R. Rivière, S. Deléglise, E. Gavartin, O. Arcizet, A. Schliesser, and T. J. Kippenberg, Science **330**, 1520 (2010).
- [11] A. H. Safavi-Naeini, T. P. M. Alegre, J. Chan, M. Eichenfield, M. Winger, Q. Lin, J. T. Hill, D. Chang, and O. Painter, Nature (London) **472**, 69 (2011).
- [12] T. P. Purdy, P.-L. Yu, R. W. Peterson, N. S. Kampel, and C. A. Regal, Phys. Rev. X **3**, 031012 (2013).
- [13] A. H. Safavi-Naeini, S. Gröblacher, J. T. Hill, J. Chan, M. Aspelmeyer, and O. Painter, Nature (London) **500**, 185 (2013).
- [14] V. Fiore, Y. Yang, M. C. Kuzyk, R. Barbour, L. Tian, and H. Wang, Phys. Rev. Lett. **107**, 133601 (2011).
- [15] X. Zhou, F. Hocke, A. Schliesser, A. Marx, H. Huebl, R. Gross, and T. J. Kippenberg, Nat. Phys. **9**, 179 (2013).
- [16] C. Dong, V. Fiore, M. C. Kuzyk, and H. Wang, Science **338**, 1609 (2012).
- [17] C. Dong, Y. Wang, and H. Wang, Natl. Sci. Rev. **2**, 510 (2015).
- [18] P. Rabl, Phys. Rev. Lett. **107**, 063601 (2011).
- [19] A. Nunnenkamp, K. Børkje, and S. M. Girvin, Phys. Rev. Lett. **107**, 063602 (2011).
- [20] M. Bhattacharya, H. Uys, and P. Meystre, Phys. Rev. A **77**, 033819 (2008).
- [21] A. Xuereb, C. Genes, and A. Dantan, Phys. Rev. Lett. **109**, 223601 (2012).
- [22] T. T. Heikkilä, F. Massel, J. Tuorila, R. Khan, and M. A. Sillanpää, Phys. Rev. Lett. **112**, 203603 (2014).
- [23] X. Xu, M. Gullans, and J. M. Taylor, Phys. Rev. A **91**, 013818 (2015).
- [24] X.-Y. Lü, Y. Wu, J. R. Johansson, H. Jing, J. Zhang,

- and F. Nori, Phys. Rev. Lett. **114**, 093602 (2015).
- [25] M.-A. Lemonde, N. Didier, and A. A. Clerk, Nat. Commun. **7**, 11338 (2016).
- [26] P.-B. Li, H.-Rong Li, and F.-L. Li, Sci. Rep. **6**, 19065 (2016).
- [27] M. Bamba and C. Ciuti, Appl. Phys. Lett. **99**, 171111 (2011).
- [28] L.-T. Shen, X.-Y. Chen, Z.-B. Yang, H.-Z. Wu, and S.-B. Zheng, Phys. Rev. A **84**, 064302 (2011).
- [29] I. Mahboob, H. Okamoto, K. Onomitsu, and H. Yamaguchi, Phys. Rev. Lett. **113**, 167203 (2014).
- [30] B. He, L. Yang, and M. Xiao, Phys. Rev. A **94**, 031802 (2016).
- [31] N. Li, J. Ren, L. Wang, G. Zhang, P. Hänggi, and B. Li, Rev. Mod. Phys. **84**, 1045 (2012).
- [32] M.D. LaHaye, J. Suh, P.M. Echternach, K.C. Schwab, and M.L. Roukes, Nature (London) **459**, 960 (2009).
- [33] D. Hatanaka, I. Mahboob, K. Onomitsu, and H. Yamaguchi, Appl. Phys. Lett. **102**, 213102 (2013).
- [34] K. Vahala, M. Herrmann, S. Knüenz, V. Batteiger, G. Saathoff, T.W. Hänsch, and Th. Udem, Nat. Phys. **5**, 682 (2009).
- [35] J.B. Khurgin, M.W. Pruessner, T.H. Stievater, and W. S. Rabinovich, Phys. Rev. Lett. **108**, 223904 (2012).
- [36] M. Eichenfeld, J. Chan, R. M. Camacho, K. Vahala, and O. Painter, Nature (London) **462**, 08524 (2009).
- [37] I. Mahboob, K. Nishiguchi, A. Fujiwara, and H. Yamaguchi, Phys. Rev. Lett. **110**, 127202 (2013).
- [38] J.D. Cohen, S.M. Meenehan, G.S. MacCabe, S. Groblacher, A.H. Safavi-Naeini, F. Marsili, M.D. Shaw, and O. Painter, Nature (London) **520**, 522 (2015).
- [39] W. Maryam, A. V. Akimou, R. P. Campion, and A. J. Kent, Nat. Commun. **4**, 2184 (2013).
- [40] I.S. Grudin, H. Lee, O. Painter, and K.J. Vahala, Phys. Rev. Lett. **104**, 083901 (2010).
- [41] A. Khaetskii, V. N. Golovach, X. Hu, and I. Žutić, Phys. Rev. Lett. **111**, 186601 (2013).
- [42] J. Kabuss, A. Carmele, T. Brandes, and A. Knorr, Phys. Rev. Lett. **109**, 054301 (2012).
- [43] H. Jing, S.K. Özdemir, X.-Y. Lü, J. Zhang, L. Yang, and F. Nori, Phys. Rev. Lett. **113**, 053604 (2014).
- [44] G. Wang, M. Zhao, Y. Qin, Z. Yin, X. Jiang, and M. Xiao, Photon. Res. **5**, 73 (2017).
- [45] See Supplemental Materials.
- [46] Y-C Liu, Y-F Xiao, Y-L Chen, X-C Yu, and Q Gong, Phys. Rev. Lett. **111**, 083601 (2013).
- [47] M.-A. Lemonde, N. Didier, and A. A. Clerk, Phys. Rev. Lett. **111**, 053602 (2013).
- [48] K. Børkje, A. Nunnenkamp, J.D. Teufel, and S.M. Girvin, Phys. Rev. Lett. **111**, 053603 (2013).
- [49] E. E. Wollman et al., Science **349**, 952 (2015).
- [50] J.-M. Pirkkalainen, E. Damskägg, M. Brandt, F. Massel, and M. A. Sillanpää, Phys. Rev. Lett. **115**, 243601 (2015).
- [51] F. Lecocq, J. B. Clark, R. W. Simmonds, J. Aumentado, and J. D. Teufel, Phys. Rev. X **5**, 041037 (2015).
- [52] J. B. Clark, F. Lecocq, R. W. Simmonds, J. Aumentado, and J. D. Teufel, arXiv:1606.08795 (2016).

Supplementary Materials

S-1. EFFECTIVE HAMILTONIAN

From the main text, we know that the Hamiltonian of the system can be written as

$$H = H_c + H_m + J \left(a_1 a_2^\dagger + a_1^\dagger a_2 \right). \quad (\text{S1})$$

For simplicity, we take the two parametric driving frequencies satisfying $\omega_{d1} = \omega_{d2} = \omega_d$. In the interaction picture $H_0 = \frac{\omega_d}{2} \left(a_1^\dagger a_1 + a_2^\dagger a_2 \right)$, the Hamiltonian of the system can be written as

$$H = \sum_{j=1}^2 \Delta_j a_j^\dagger a_j + \Lambda_j \left(a_j^{\dagger 2} e^{-i\Phi_{dj}} + \text{H.c.} \right) + \omega_m b^\dagger b - g_0 a_2^\dagger a_2 (b^\dagger + b) + J \left(a_1 a_2^\dagger + a_1^\dagger a_2 \right), \quad (\text{S2})$$

where the detuning $\Delta_j = \omega_j - \omega_d/2$.

To diagonalize the H_c , we introduce a squeezing transformation [S1]

$$a_j = \cosh(r_{dj}) a_{sj} - e^{-i\Phi_{dj}} \sinh(r_{dj}) a_{sj}^\dagger, \quad (\text{S3})$$

where

$$r_{dj} = 1/4 \ln [(\Delta_j + 2\Lambda_j) / (\Delta_j - 2\Lambda_j)], \quad (\text{S4})$$

which requires $|\Delta_j| > |2\Lambda_j|$ to avoid the system instable.

The Hamiltonian of the system can be changed into

$$\begin{aligned} H = & \sum_{j=1}^2 \omega_{sj} a_{sj}^\dagger a_{sj} + \omega_m b^\dagger b - g_{s2} a_{s2}^\dagger a_{s2} (b^\dagger + b) + g_{p2} \left(e^{-i\Phi_{d2}} a_{s2}^{\dagger 2} + \text{H.c.} \right) (b^\dagger + b) \\ & + J \left(\lambda_1 a_{s1} a_{s2}^\dagger - \lambda_2 a_{s1} a_{s2} + \text{H.c.} \right) - F (b^\dagger + b) + C \end{aligned} \quad (\text{S5})$$

where

$$\omega_{sj} = (\Delta_j - 2\Lambda_j) \exp(2r_{dj}), \quad (\text{S6})$$

$$g_{s2} = g_0 \left[\sinh^2(r_{d2}) + \cosh^2(r_{d2}) \right] = \frac{g_0 \Delta_2}{\sqrt{\Delta_2^2 - 4\Lambda_2^2}}, \quad (\text{S7})$$

$$g_{p2} = g_0 \cosh(r_{d2}) \sinh(r_{d2}) = \frac{g_0 \Lambda_2}{\sqrt{\Delta_2^2 - 4\Lambda_2^2}}, \quad (\text{S8})$$

$$\lambda_1 = \cosh(r_{d1}) \cosh(r_{d2}) + \sinh(r_{d1}) \sinh(r_{d2}) e^{i(\Phi_{d1} - \Phi_{d2})}, \quad (\text{S9})$$

$$\lambda_2 = \cosh(r_{d1}) \sinh(r_{d2}) e^{i\Phi_{d2}} + \sinh(r_{d1}) \cosh(r_{d2}) e^{i\Phi_{d1}}, \quad (\text{S10})$$

$$F = g_0 \sinh^2(r_{d2}), \quad (\text{S11})$$

$$C = \sum_{j=1}^2 \Delta_j \sinh^2(r_{dj}) - 2\Lambda_j \cosh(r_{dj}) \sinh(r_{dj}). \quad (\text{S12})$$

S-2. PHASE-CONTROLLED OPTOMECHANICAL SYSTEMS WITH $f_1 \gg 1$

With the rotating approximation, we can eliminate the term $\lambda_1 a_{s1} a_{s2}^\dagger + \text{H.c.}$ when we have

$$f_1 \equiv \left| \frac{\lambda_2 (\omega_{s1} - \omega_{s2})}{\lambda_1 (\omega_{s1} + \omega_{s2})} \right| \gg 1, \quad (\text{S13})$$

which means that the effective interaction from squeezing terms is much larger. It is obvious that only the squeezing terms can be reserved to enhance optomechanical coupling strength [S2].

Similar to the above, we can diagonalize the two-mode squeezing via the squeezing transformation [S2]

$$a_{sj} = \cosh(r) A_j - e^{-i\Phi} \sinh(r) A_k^\dagger (j \neq k), \quad (\text{S14})$$

where

$$r = \frac{1}{4} \ln [(\omega_{s1} + \omega_{s2} + |J'|) / (\omega_{s1} + \omega_{s2} - |J'|)], \quad (\text{S15})$$

in which $J' = 2J\lambda_2$ and $\Phi = \arg(J')$. To avoid the system instability, we need

$$f_2 \equiv |\omega_{s1} + \omega_{s2}| - |J'| > 0. \quad (\text{S16})$$

This leads to the following Hamiltonian

$$\begin{aligned} H = & \omega_m b^\dagger b + \sum_{j=1}^2 W_j A_j^\dagger A_j - G_j A_j^\dagger A_j (b^\dagger + b) + \sum_{j \leq k=1}^2 (G_{jk} A_j A_k + \text{H.c.}) (b^\dagger + b) \\ & - (G_{p12} A_1^\dagger A_2 + \text{H.c.}) (b^\dagger + b) + (F' - F) (b^\dagger + b) + C + C', \end{aligned} \quad (\text{S17})$$

where

$$W_1 = \omega_{s1} \cosh^2(r) + \omega_{s2} \sinh^2(r) - |J'| \sinh(2r) / 2, \quad (\text{S18})$$

$$W_2 = \omega_{s2} \cosh^2(r) + \omega_{s1} \sinh^2(r) - |J'| \sinh(2r) / 2, \quad (\text{S19})$$

$$G_1 = g_0 \cosh(2r_{d2}) \sinh^2(r), \quad (\text{S20})$$

$$G_2 = g_0 \cosh(2r_{d2}) \cosh^2(r), \quad (\text{S21})$$

$$G_{12} = \frac{g_0}{2} e^{i\Phi} \cosh(2r_{d2}) \sinh(2r), \quad (\text{S22})$$

$$G_{11} = \frac{g_0}{2} e^{i(2\Phi - \Phi_{d2})} \sinh(2r_{d2}) \sinh^2(r), \quad (\text{S23})$$

$$G_{22} = \frac{g_0}{2} e^{i\Phi_{d2}} \sinh(2r_{d2}) \cosh^2(r), \quad (\text{S24})$$

$$G_{p12} = \frac{g_0}{2} e^{i(\Phi_{d2} - \Phi)} \sinh(2r_{d2}) \sinh(2r), \quad (\text{S25})$$

$$F' = g_0 \cosh(2r_{d2}) \sinh^2(r), \quad (\text{S26})$$

$$C' = (\omega_{s2} + \omega_{s1}) \sinh^2(r) - |J'| \sinh(r) \cosh(r). \quad (\text{S27})$$

We notice that $F' - F$ and $C + C'$ are only the displaced term and a constant, respectively, which can be neglected in the optomechanical system.

We have discussed the radiation-pressure optomechanical coupling in the main text. With the appropriate parameters, the parametric amplification coupling forms can also be obtained.

To obtain the effective Hamiltonian, we notice that there are the following conditions: (a) $f_1 \gg 1$ (rotating wave approximation); (b) $|\Delta_j| > |2\Lambda_j|$ and $f_2 > 0$ (stable conditions). Naturally, the system parameters are chosen to satisfy $|\Delta_j| > |2\Lambda_j|$. Equipotential lines $f_1 = 10$ (blue line) and $f_2 = 0$ (red line) versus Λ_1 and $\Delta\Phi$ are plotted in Fig. S1(a), and the area between the blue and red lines fully satisfies the above conditions. In Fig. S1(b), we plot the coupling G_2/ω_m (red-dashed line) and G_{12}/ω_m (blue-solid line) versus phase difference $\Delta\Phi$, and we can reach the strong-coupling regime when $\Delta\Phi = \pi$, however, which is much smaller than the mechanical frequency ω_m . The supermode frequencies $|W_1|/\omega_m$ (red-solid line) and W_2/ω_m (blue-dashed line) are shown in Fig. S1(c), which means that we have $\omega_m \gg G_j$, $|2W_j \pm \omega_m| \gg |G_{jj}|$ and $|W_1 - W_2 \pm \omega_m| \gg |G_{p12}|$. While we find the frequency matching (red square points) $|W_1 + W_2 - \omega_m| \approx 0$ in Fig. S1(d), which leads that only the term G_{12} can be reserved. It is obvious that we can also obtain the parametric amplification coupling forms when $|2W_j \pm \omega_m| \approx 0$ with appropriate parameters.

When only one parametric driving field exists in the cavity, we can still realize enhanced optomechanical coupling without phase control. If the parametric driving field exists in the second cavity, it means $\Lambda_1 = 0$ ($r_{d1} = 0$), and all coupling forms are same to the above. The phase difference does not appear in the expression of effective coupling $|J'| = 2J \sinh(r_{d2})$, which means the coupling parameters can not be tuned by the phase difference. It needs a stronger photon-hopping interaction J because of no product factor $\sinh(r_{d1})$ or $\cosh(r_{d1})$ in the effective $|J'|$. We

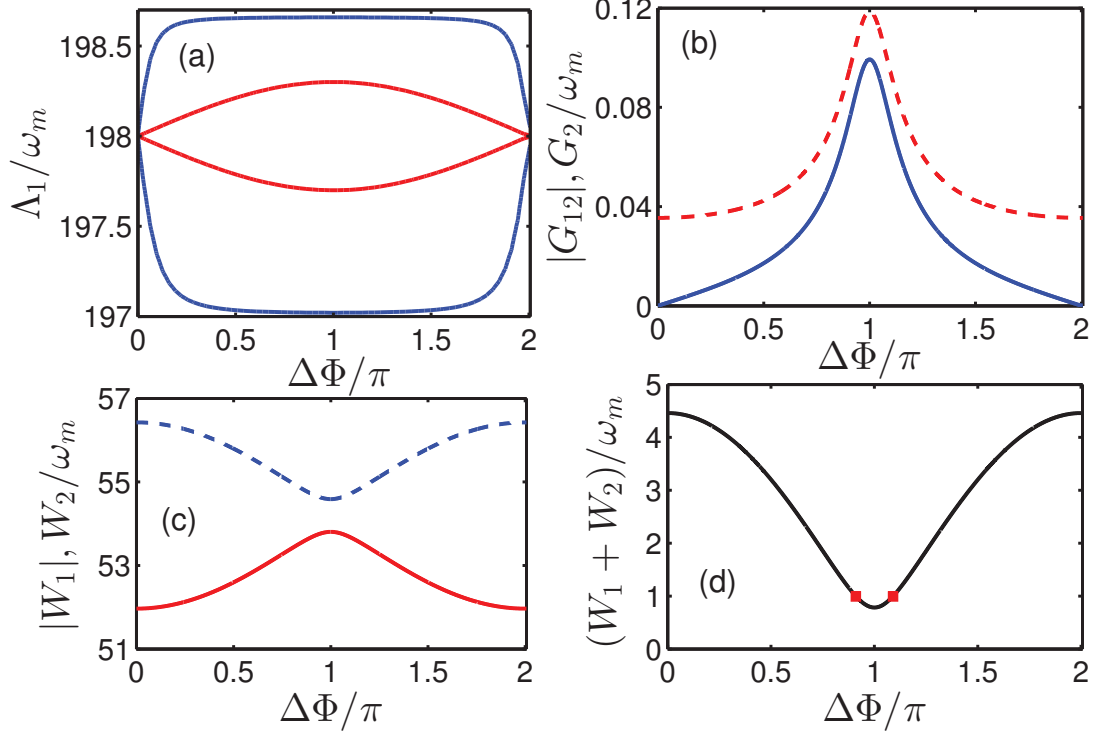


FIG. S1: (Color online) (a) Equipotential lines $f_1 = 10$ (blue line) and $f_2 = 0$ (red line) versus Λ_1 and $\Delta\Phi$. (b) The coupling G_2/ω_m (red-dashed line) and G_{12}/ω_m (blue-solid line) versus phase difference $\Delta\Phi$. (c) The supermodes $|W_1|/\omega_m$ (red-solid line) and W_2/ω_m (blue-dashed line) versus phase difference $\Delta\Phi$. (d) The frequency $(W_1 + W_2)/\omega_m$ versus phase difference $\Delta\Phi$. The red square points show the resonant condition $W_1 + W_2 = \omega_m$. The parameters are $\Delta_1 = -400\omega_m$, $\Delta_2 = 400\omega_m$, $\Lambda_1 = 198.305\omega_m$, $\Lambda_2 = 198\omega_m$, $g_0 = 0.005\omega_m$, $J = 0.3\omega_m$, and $\kappa = 0.05\omega_m$.

can still realize the controlled optomechanical coupling by tuning Λ_2 , Δ_j and J . If the parametric driving field exists in the first cavity, we have $\Lambda_2 = 0$ ($r_{d2} = 0$). The coupling strength becomes $G_1 = g_0 \sinh^2(r)$ and $G_2 = g_0 \cosh^2(r)$, and the enhanced optomechanical coupling can still be obtained. The OPA is put into the auxiliary cavity, which may be easier to implement in the experiment.

S-3. PHASE-CONTROLLED PHONON LASER WITH $f_1 \ll 1$

When $f_1 \ll 1$, we can neglect the term $\lambda_2 a_{s1}^\dagger a_{s2}^\dagger + \text{H.c.}$ (rotating wave approximation), and the Hamiltonian of the system can be written as

$$\begin{aligned}
 H = & \sum_{j=1}^2 \omega_{sj} a_{sj}^\dagger a_{sj} + \omega_m b^\dagger b - g_{s2} a_{s2}^\dagger a_{s2} (b^\dagger + b) + g_{p2} \left(e^{-i\Phi} a_{s2}^\dagger a_{s2}^\dagger + \text{H.c.} \right) (b^\dagger + b) \\
 & + J \left(\lambda_1 a_{s1} a_{s2}^\dagger + \text{H.c.} \right) - F (b^\dagger + b) + C,
 \end{aligned} \tag{S28}$$

To diagonalize the interaction term λ_1 , we introduce the transformation

$$a_{s1} = \cos\left(\frac{\theta}{2}\right) A_1 + e^{-i\Phi} \sin\left(\frac{\theta}{2}\right) A_2, \tag{S29}$$

$$a_{s2} = \cos\left(\frac{\theta}{2}\right) A_2 - e^{i\Phi} \sin\left(\frac{\theta}{2}\right) A_1, \tag{S30}$$

where $\theta = \arctan\left(\frac{|J'|}{\omega_{s2} - \omega_{s1}}\right)$, in which $J' = 2J\lambda_1$ and $\Phi = \arg(J')$.

The Hamiltonian can be written as

$$\begin{aligned}
H = & \omega_m b^\dagger b + \sum_{j=1}^2 W_j A_j^\dagger A_j - G_j A_j^\dagger A_j (b^\dagger + b) + \sum_{j \leq k=1}^2 (G_{jk} A_j A_k + \text{H.c.}) (b^\dagger + b) \\
& + (G_{p12} A_1^\dagger A_2 + \text{H.c.}) (b^\dagger + b) - F (b^\dagger + b) + C,
\end{aligned} \tag{S31}$$

where

$$W_1 = \omega_{s1} \cos^2 \left(\frac{\theta}{2} \right) + \omega_{s2} \sin^2 \left(\frac{\theta}{2} \right) - |J'| \sin(\theta) / 2, \tag{S32}$$

$$W_2 = \omega_{s2} \cos^2 \left(\frac{\theta}{2} \right) + \omega_{s1} \sin^2 \left(\frac{\theta}{2} \right) + |J'| \sin(\theta) / 2, \tag{S33}$$

$$G_1 = g_0 \cosh(2r_{d2}) \sin^2 \left(\frac{\theta}{2} \right), \tag{S34}$$

$$G_2 = g_0 \cosh(2r_{d2}) \cos^2 \left(\frac{\theta}{2} \right), \tag{S35}$$

$$G_{12} = -\frac{g_0}{2} e^{i(\Phi_{d2} + \Phi)} \sinh(2r_{d2}) \sin(\theta), \tag{S36}$$

$$G_{11} = \frac{g_0}{2} e^{i(2\Phi + \Phi_{d2})} \sinh(2r_{d2}) \sin^2 \left(\frac{\theta}{2} \right), \tag{S37}$$

$$G_{22} = \frac{g_0}{2} e^{i\Phi_{d2}} \sinh(2r_{d2}) \cos^2 \left(\frac{\theta}{2} \right), \tag{S38}$$

$$G_{p12} = \frac{g_0}{2} e^{-i\Phi} \cosh(2r_{d2}) \sin(\theta). \tag{S39}$$

We know that the phonon laser can be realized by the Hamiltonian

$$H = \omega_m b^\dagger b + \sum_{j=1}^2 W_j A_j^\dagger A_j + G_{p12} A_1^\dagger A_2 b + \text{H.c.}, \tag{S40}$$

when we have $\omega_m \gg G_j$, $|W_j + W_k \pm \omega_m| \gg |G_{jk}|$ and $|W_1 - W_2 \pm \omega_m| \approx 0$.

In Fig. S2(a), we plot the equipotential lines $f_1 = 0.1$ (blue line) versus A_1 and $\Delta\Phi$, and the area between the blue and red lines fully satisfies $f_1 \ll 1$. The frequencies W_1/ω_m (red-dashed line), W_2/ω_m (blue-dashed line), and $(W_1 - W_2)/\omega_m$ (blue-solid line) are shown in Fig. S2(b). We find the frequency matching (red square points) $|W_1 - W_2 - \omega_m| \approx 0$, which leads that only the term G_{p12} can be reserved. While the rotating wave approximation is satisfied, we can realize the phase-controlled phonon laser. In Fig. S2(b), the frequency $|2W_2 - \omega_m| \approx 0$ can also be matched, which is denoted by the green dots. It is obvious that we can obtain the parametric amplification coupling form G_{22} only by the tuning phase difference.

* Electronic address: jinghui73@gmail.com

† Electronic address: xbz@ustc.edu.cn

[S1] X.-Y. Lü, Y. Wu, J. R. Johansson, H. Jing, J. Zhang, and F. Nori, Phys. Rev. Lett. **114**, 093602 (2015).

[S2] P.-B. Li, H.-R. Li, and F.-L. Li, Sci. Rep. **6**, 19065 (2016).

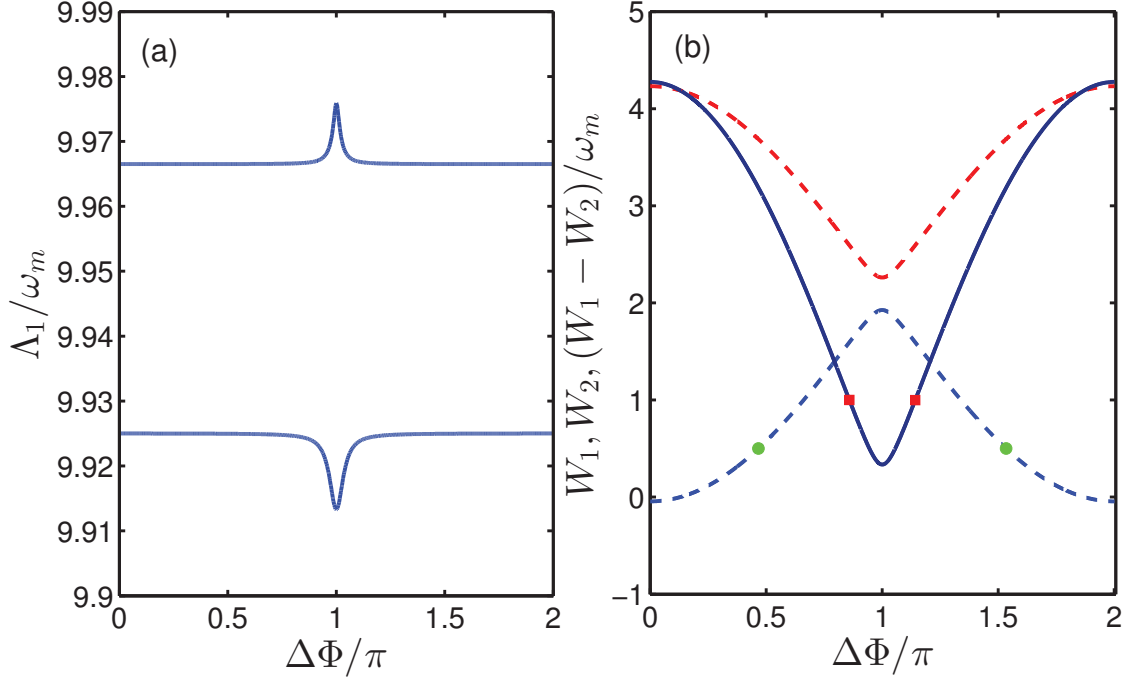


FIG. S2: (Color online) (a) Equipotential lines $f_1 = 0.1$ versus Λ_1 and $\Delta\Phi$. (b) The coupling G_2/ω_m (red-dashed line) and G_{12}/ω_m (blue-solid line) versus phase difference $\Delta\Phi$. (c) The frequencies W_1/ω_m (red-dashed line), W_2/ω_m (blue-dashed line), and $(W_1 - W_2)/\omega_m$ versus phase difference $\Delta\Phi$. The red square points and green dots show the resonant condition $W_1 - W_2 = \omega_m$ and $W_2 = 0.5\omega_m$, respectively. The other parameters are $\Delta_1 = 20\omega_m$, $\Delta_2 = 100\omega_m$, $\Lambda_1 = 9.94\omega_m$, $\Lambda_2 = 49.99\omega_m$, $g_0 = 0.002\omega_m$, $J = 0.1\omega_m$, and $\kappa = 0.05\omega_m$.